

## The de Haas-van Alphen Effect of Zinc

著者	FUKUROI Tadao, SAITO Yoshitami
journal or publication title	Science reports of the Research Institutes, Tohoku University. Ser. A, Physics, chemistry and metallurgy
volume	9
page range	273-292
year	1957
URL	<a href="http://hdl.handle.net/10097/26832">http://hdl.handle.net/10097/26832</a>

# The de Haas-van Alphen Effect of Zinc\*

Tadao FUKUROI and Yoshitami SAITO

*The Research Institute for Iron, Steel and Other Metals*

(Received May 23, 1957)

## Synopsis

The de Haas-van Alphen effect of pure zinc crystal was investigated at temperatures ranging from 63° to 1.3°K by means of a torsion magnetometer. In the magnetic field less than 16 kilo-oersted and at the temperatures 4.2°K and above, a remarkable periodic variation of magnetic susceptibility was found with the intensity of magnetic field and it is here referred to as the long-period effect. While in the field higher than 19 kilo-oersted and at temperatures from 4.2° to 1.3°K, it was observed that a shorter-period and smaller-amplitude effect, which is accompanied by some complicated beat structures, is superposed on the high field extension of the long-period effect just cited. From the analysis of the long-period effect, we obtained the next de Haas-van Alphen parameters:  $E_{0l} = 5.5 \times 10^{-14}$  erg,  $m_{1l}/m_0 = 5.4 \times 10^{-3}$ ,  $m_{3l}/m_0 = 2.7 \times 10^{-1}$ ,  $T_{Dl} = 400^\circ\text{K}$ ,  $n_l = 1.2 \times 10^{-6}$  atom $^{-1}$ ; and from the analysis of the short-period effect, we got:  $E_{0s} = 7.9 \times 10^{-14}$  erg,  $m_{1s}/m_0 = 1.6 \times 10^{-1}$ ,  $m_{3s}/m_0 = 8.3 \times 10^{-2}$ ,  $T_{Ds} = 570^\circ\text{K}$ ,  $n_s = 3 \times 10^{-5}$  atom $^{-1}$ .

## I. Introduction

The appearance of approximately periodic variation of the magnetic susceptibility of bismuth at very low temperatures and under a strong magnetic field is an effect discovered by de Haas and van Alphen in 1930. At that time, it was considered to be an effect specific to bismuth in view of the peculiar characteristics of this metal, but since Peierls<sup>(1)</sup> and Blackman<sup>(2)</sup> have developed a theory on the effect basing on a free electron model, this effect has become known as a more general phenomenon to be found possibly in other metals too. Since then, some advance has been made in the theoretical side, but owing to the imperfectness of the experimental apparatus together with the difficulty in measurement, the observation of this effect in other metals was not successful for a long time.

More recently, since Marcus<sup>(3)</sup> detected the de Haas-van Alphen effect (referred to hereafter as dH-vA effect) in zinc in 1947, the experimental studies on this problem have been stimulated, and to date, the effect has been observed in graphite and 14 kinds of metals including mercury.<sup>(4,5,6)</sup>

A relatively large number of reports have been published on the effect in zinc. In chronological order, the outstanding works are as follows. The first experiment by Marcus was made by Faraday's method at the temperature of 20°K in a mag-

\* The 884th report of the Research Institute for Iron, Steel and Other Metals.

- (1) R. Peierls, *Z. f. Phys.*, **81** (1933), 186.
- (2) M. Blackman, *Proc. Roy. Soc. London*, **A166** (1938), 1.
- (3) J. A. Marcus, *Phys. Rev.*, **71** (1947), 559.
- (4) D. Shoenberg, *Nature*, **167** (1951), 647.
- (5) D. Shoenberg, *Nature*, **170** (1952), 569.
- (6) D. Shoenberg, *Trans. Roy. Soc. London*, **A 245** (1952), 1.

netic field up to 11 kilo-gauss (kG) and the maxima were found at 5.3 kG and 9.3 kG and the minimum at 7.1 kG. By 1951, he gave out four reports<sup>(7)~(10)</sup>, in one of which (1950), he measured the effect in Zn-Cu and Zn-Al alloys and made the statement noticeable from the point of view of the electron theory of dilute alloys that in Zn-Cu alloy (Cu: 0.32 at. %) the peaks representing the maxima and the minima of oscillation are shifted to the side of high magnetic field and the amplitude increases on the side of high and decreases on the side of low magnetic field in comparison with the case of pure zinc, while in Zn-Al alloy (Al: 0.26 at. %) both the period and the amplitude are reduced at any strength of the magnetic field. In 1949, Sydoriak and Robinson<sup>(11)</sup> made experiments at 4.2°K~20°K and 8.5 kG and Mackinnon<sup>(12)</sup> at 1.4°K~4.2°K and 8 kG respectively to some details and determined many dH-vA parameters, but the results are discrepant to a considerable extent by the authors.

Unlike in other metals, in zinc the effect is observable even at relatively high temperature range. It is another characteristic of the effect in zinc that, in the face of the theoretically expected independence of the periods with the variation of temperature, the period is highly dependent on temperature in this metal. Clure and Marcus<sup>(10)</sup> first observed this temperature dependence and Berlincourt and Steele<sup>(13)</sup> have made a detailed investigation on it.

In the studies cited above, measurements were made under relatively weak magnetic fields and only one simple sort of period was observed. Berlincourt and Steele<sup>(13)</sup> extended the experimental magnetic fields up to 25 kG and found a shorter period appearing in the range of stronger magnetic fields, but did not touch upon it in detail. On the influence of impurities on the dH-vA effect too, there seems to be little elucidation, though beside the above cited report by Marcus, some studies have been made on bismuth<sup>(14)</sup> and tin,<sup>(15)</sup> so that it is far from easy to obtain informations on the dH-vA effect with anything like adequate completeness. In consideration of such a situation, we have carried out measurements of the dH-vA effect of pure zinc crystal mainly in strong magnetic fields ranging from 19 kG to 26 kG at liquid helium temperatures and investigated the details of the short-period effect found only under strong magnetic fields.

## II. Apparatus and specimens used in the measurements

### 1. Apparatus

In the earlier experiments on the effect, the Faraday's method was generally used, but in this method, as the specimens have to be placed in a non-uniform

(7) J. A. Marcus, *Phys. Rev.*, **76** (1949), 413.

(8) J. A. Marcus, *Phys. Rev.*, **76** (1949), 621.

(9) J. A. Marcus, *Phys. Rev.*, **77** (1950), 750.

(10) M. C. Clure and J. A. Marcus, *Phys. Rev.*, **84** (1951), 787.

(11) S. G. Sydoriak and J. E. Robinson, *Phys. Rev.*, **75** (1949), 118.

(12) E. Mackinnon, *Proc. Phys. Soc.*, **B62** (1949), 170.

(13) T. G. Berlincourt and M. C. Steele, *Phys. Rev.*, **95** (1954), 1421.

(14) D. Shoenberg, *Proc. Roy. Soc. London*, **A170** (1939), 341.

(15) G. T. Croft, W. F. Love and F. C. Nix, *Phys. Rev.*, **95** (1954), 1403.

field, the strength of the magnetic field is not equal in all the parts of the specimen, so that the oscillation, especially of short-period, is apt to be smeared out. Since 1939, first due to Shoenberg, the method of measuring the torque in a uniform field which is attributable to the anisotropy in magnetic susceptibility of a single crystal has come into general use.

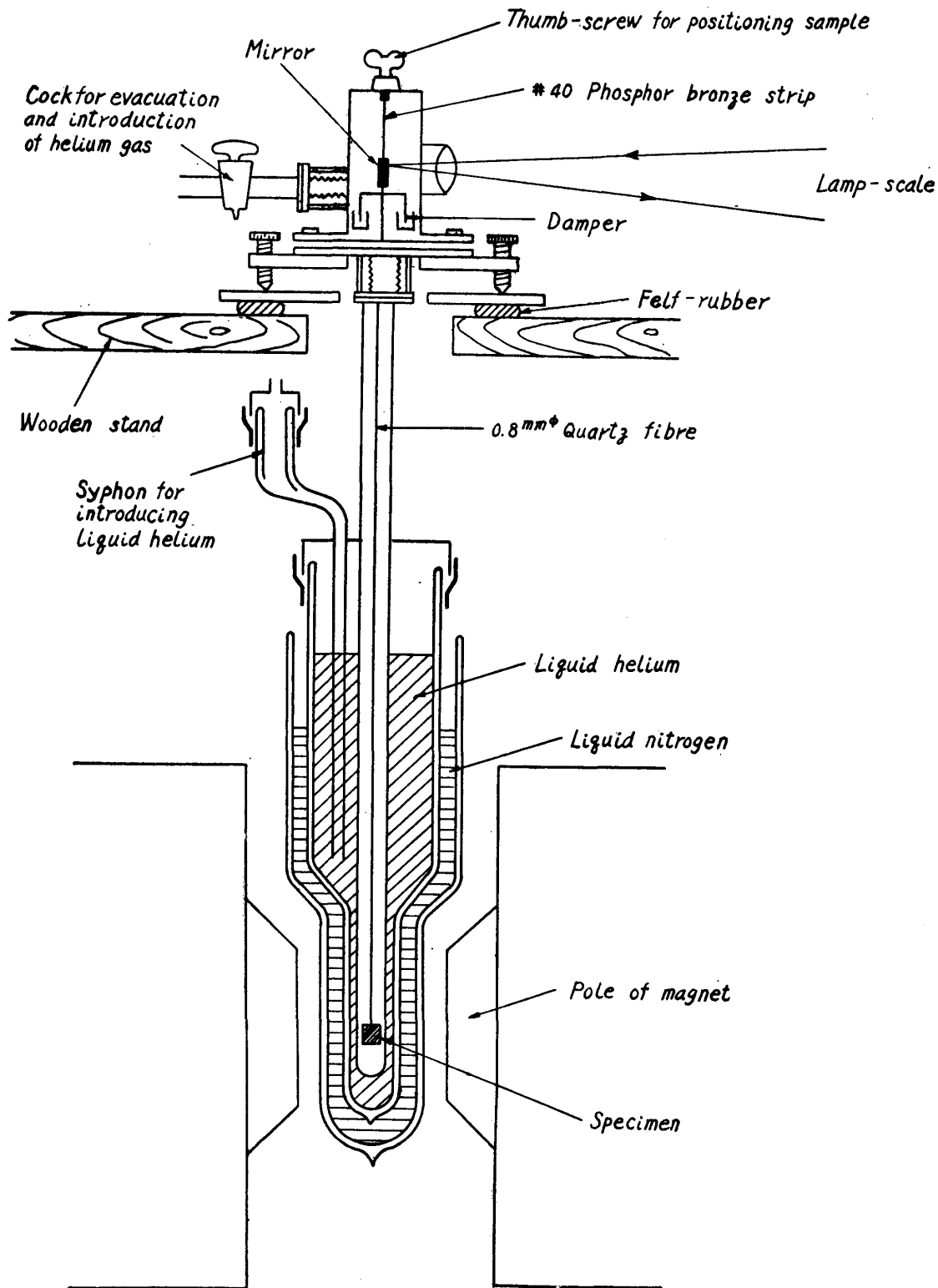


Fig. 1. Experimenting apparatus: the transferable torque magnetometer.

By this torsion method, it is feasible to measure the difference of the magnetic susceptibility in two mutually perpendicular directions with a great deal of accuracy. The schema of the apparatus used in our measurements is shown in Fig. 1. In order to keep off the external vibration which disturbs the results of measurement, we placed sand-boxes and 96 sponge-rubber balls under the stand supporting the torsion magnetometer and a Dewar vessel, along with a felt-rubber plate between the magnetometer and the stand. A mirror, a damper immersed in liquid paraffin and a torsion fibre are suspended from an aluminium piece attached on to the screw for adjusting the position of the specimen. The specimen was affixed with cemedine on a small circular disk at the lower end of a thin quartz rod of about 0.8 mm in diameter.

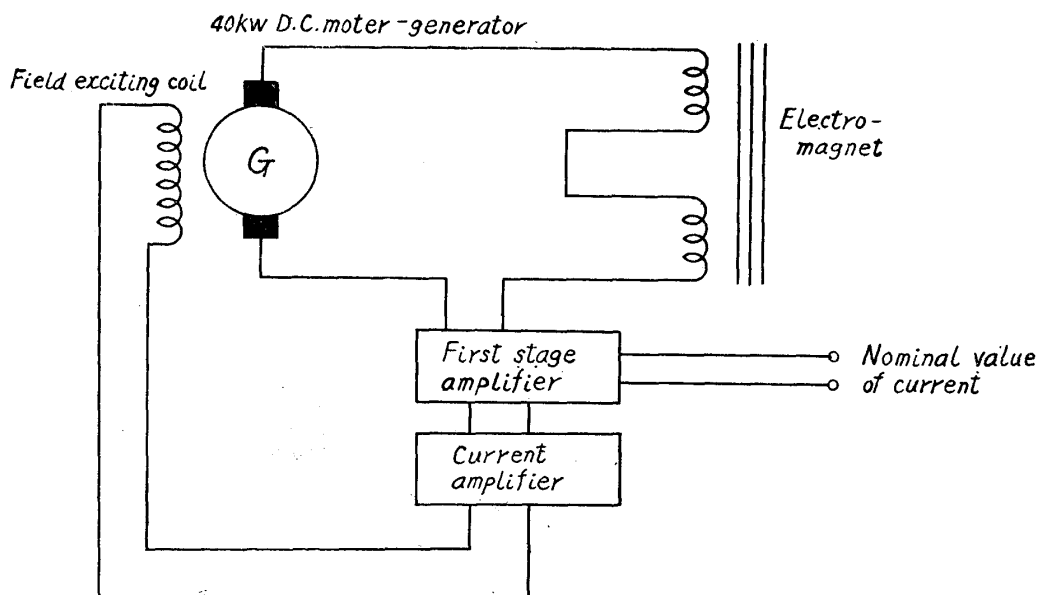


Fig. 2. Regulating circuit of the magnetizing current.

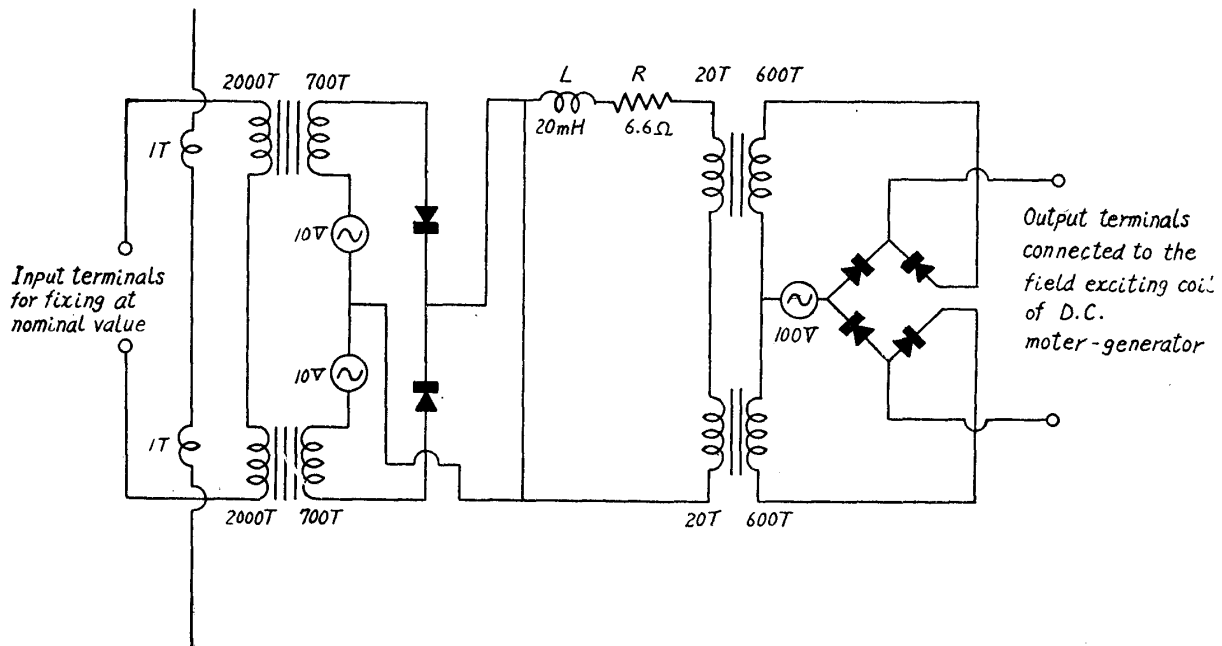


Fig. 3. Magnetic amplifier circuit for field exciting current of the motor-generator.

2. Magnetic field

With a large-size electromagnet of 40 kW capacity and 10 tons in weight, a maximum field of 26 kG was attained by flowing a current of 200 A. The block diagrams of the control and stabilizing circuits of the magnetizing current and the magnetic-amplifier are shown in Figs. 2 and 3. By these devices, we could stabilize the current fluctuation less than 0.1 per cent against a 10 per cent change in the voltage of the load resistance power source.

3. Specimens

By the Bridgman's method, a rod-form single crystal of 5mm diameter was prepared and a specimen of about 4 mm both in length and in diameter was cut out of it, weighing 0.330 g. Chemical analysis revealed impurity contents in the single crystal as shown in Table 1. For orienting the crystal axes of the specimen, we have used the light figure method.

Table 1. Impurities involved in zinc crystals (Chemical analysis)

Element	Per cent
Pb	0.0017
Cd	0.0001
Sb	none
Cu	0.0002
Sn	none
S	none
As	none
Fe	0.0008
Resultant purity 99.996%	

4. Method of measurement

Let us denote the direction [0001] of the single crystal by axis-3, the two other directions  $[\bar{1}2\bar{1}0]$  and  $[\bar{1}010]$ , lying in the plane perpendicular to axis-3 and mutually perpendicular, by axis-2 and axis-1, and the magnetic susceptibility in the three directions by  $\chi_3$ ,  $\chi_2$  and  $\chi_1$ , respectively.

The torque acting upon the specimen having the general orientation of which the Eulerian angles are  $(\theta, \psi$  and  $\phi)$  as shown in Fig. 4, is given by the next expression.

$$\begin{aligned}
 C = & \{ \chi_3 \sin^2 \phi - (\chi_1 \sin^2 \psi + \chi_2 \cos^2 \psi) \} mH^2 \sin \theta \cos \theta \\
 & + (\chi_2 \sin^2 \psi + \chi_1 \cos^2 \psi) mH^2 \cos^2 \phi \sin \theta \cos \theta \\
 & + (\chi_2 - \chi_1) (\cos^2 \theta - \sin^2 \theta) mH^2 \sin \phi \cos \phi \cos \theta.
 \end{aligned}
 \tag{1}$$

For facilitating the analysis of the experimental results, it is desirable to set the specimens in the position with the axis-3 horizontal and either the axis-2 or the axis-1 vertical ( $\phi = 90^\circ$ , Fig. 5(a)) and in the position with axis-3 vertical ( $\phi = 0$ , Fig. 5(b)). Such being the case, owing to the difficulty in setting the specimen exactly in such a position, we obliged to fix the specimen at the positions with the axis-2 deviating by  $8.2^\circ$  from the vertical (Fig. 5(c)) and with the axis-3

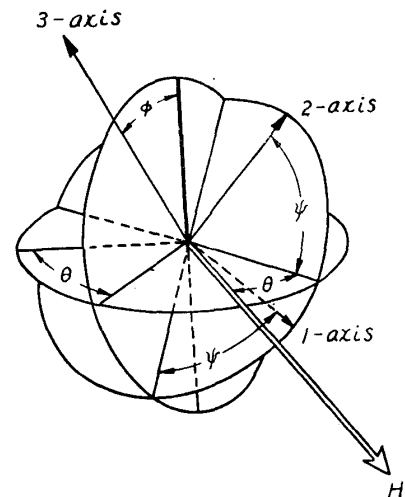


Fig. 4. Most general orientation of the specimen crystal.

deviating by about  $0^{\circ}40'$  from the vertical (Fig. 5(d)).

On assuming that the magnetic susceptibility in the basal plane perpendicular to the axis-3 is isotropic for the time being (on this point, see below), the torque\*

due to the magnetic field in the position given in Fig. 5(c) would become

$$C = \frac{1}{2}mH^2(\chi_3 - \chi_1)\sin 2(\theta - \alpha), \quad (2)$$

where  $\theta$  stands for the angle between the axis-3 and the magnetic field,  $\alpha$  for the angle of deflection of mirror and  $m$  for the mass of the specimen. When the shift of the image, i.e., the deflection of the mirror, is small, the correction term may be disregarded. With the torsion fibre we used, 2.40 cm in length and with the torsion constant of 41.45 dyne cm/radian, when the distance between the mirror and its image is taken at 141.9 cm, 1 mm shift of the image corresponds to the torque of

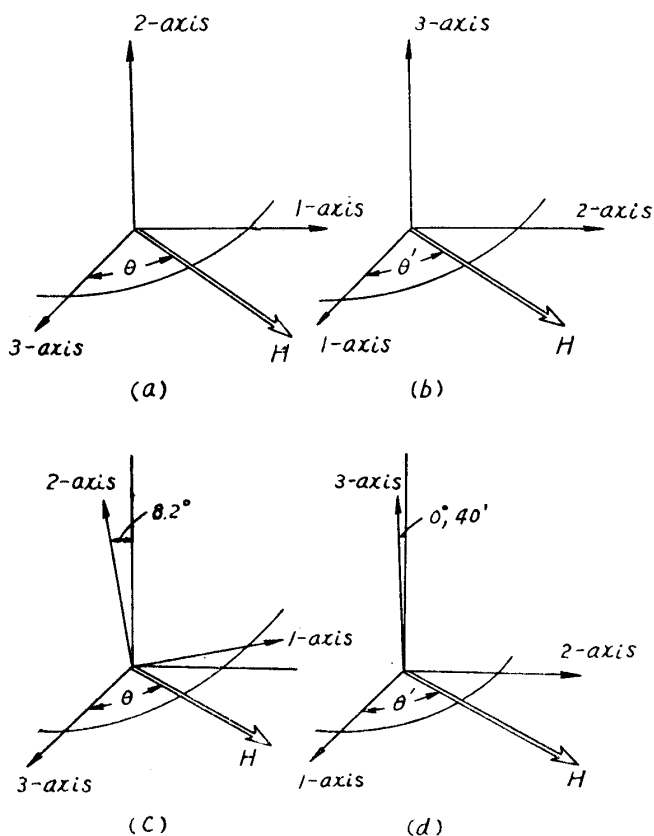


Fig. 5. Specific orientations of the specimen crystal.

$$C_{1mm} = 1.463 \times 10^{-2} \text{ dyne cm.} \quad (3)$$

Therefore, when the shift of the image is denoted by  $\Delta l$  (cm), the strength of the magnetic field by  $H$  (gauss) and the mass of the specimen by  $m$  (g), the difference of susceptibility along two perpendicular directions  $\Delta\chi$  is given by

$$\Delta\chi = 0.2926 \cdot \frac{1}{m} \cdot \frac{\Delta l}{H^2} \cdot \frac{1}{\sin 2(\theta - \alpha)} \text{ cgsemu.} \quad (4)$$

In measuring the torque, special care should be taken for the presence of ferro-magnetic impurities. If the system suspending the specimen contains some ferro-magnetic impurities, the torque would comprise, besides the 2-cycled term given by Equ. (2), a term  $\sum M_i H \sin \theta_i$  due to the localization of the magnetic moment  $M_i$  in addition. Here  $\theta_i$  stands for the angle between  $M_i$  and  $H$ . In this case the torque curve would contain a 1-cycled term beside the 2-cycled terms. This gives a sensitive indication of the presence of ferro-magnetic impurities.

\* The maximum shift 24 cm (Fig. 17) in the plane of axes-2 and -1 is equivalent to  $|\chi_1 - \chi_2| = 4.7 \times 10^{-8}$ . When we use  $f(\psi)$  for  $\chi_1 \sin_2 \psi + \chi_2 \cos_2 \psi$  in the first term of Equ.(1), the calculated value of  $\frac{|f(90^\circ - 8.2^\circ) - f(90^\circ)|}{f(90^\circ - 8.2^\circ)}$  falls smaller than 0.007. Therefore, the deviation of  $8.2^\circ$  of the axis-2 from the vertical direction would cause an error not larger than 0.1 per cent, so that we may assume Equ. (2) as the formula to determine the torque.

### III. Results of measurement

For convenience of descriptions, the results will be described under four different sets of conditions, concerning the range of measurements and the orientation of the specimen, as follows:

(A) In the vicinity of the highest temperature where the oscillatory phenomenon is observable (temperature range of liquid nitrogen);

(B) In the range of  $4.2^\circ\text{K}$  in temperature and above 16 kG of magnetic field (Long-period effect);

(C) In the range of  $4.2^\circ\text{K} \sim 1.3^\circ\text{K}$  and above 19 kG (Short-period effect);

(D) With the specimen suspended along the axis-3 vertical, i. e. the procedure to detect the susceptibility difference in the hexagonal base plane by rotating the magnet with respect to the crystal in the horizontal plane, while keeping the intensity of magnetic field constant.

#### 1. Results of measurement at the temperature of liquid nitrogen

A part of the results of measurements at  $63^\circ\text{K}$  obtained by lowering the vapour pressure of liquid nitrogen and varying the angle  $\theta$  are shown in Figs. 6(a), (b) and (c). Within the range up to 15 kG only 3 peaks of maxima and minima of oscillation are observable. That is to say, the period is very long. The amplitude of oscillation tends to diminish as the angle  $\theta$  between axis-3 and the magnetic field is increased and the period becomes almost unobservable when  $\theta$  nears  $60^\circ$ . We cannot yet draw quantitative conclusions on the dependence of the period on the angle  $\theta$ , as the number of the observed peaks was too small, but it can be said that the period tends to diminish with the increase of  $\theta$ . Fig. 6 (d) shows the result of measurements at room temperature, from which we see that the difference susceptibility  $\Delta\chi$  is independent of the magnetic field. In Fig. 6 (e) is shown the angular dependence of  $\Delta\chi$  at  $290^\circ\text{K}$  and under constant magnetic field ( $H = 2,960 \text{ G}$ ). Inasmuch as zinc has two-fold rotation symmetry when the axis-3 is kept horizontal, it is expected that a  $180^\circ$  cycle will be found. The absence of the terms other than 2-cycled term in the torque curve in this position proves that the specimen contains no

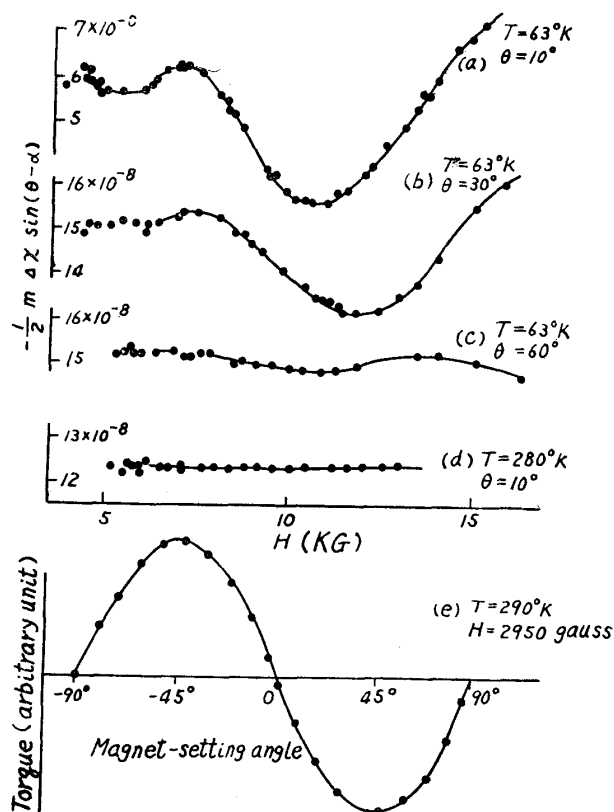


Fig. 6. Results at room temperature and at temperatures available with liquid nitrogen.



or negligible ferromagnetic impurity, if any.

2. Results of measurements at 4.2°K and up to 16 kG (Long-period effect)

As in (A) above, measurements were made at various angles  $\theta$ , of which the

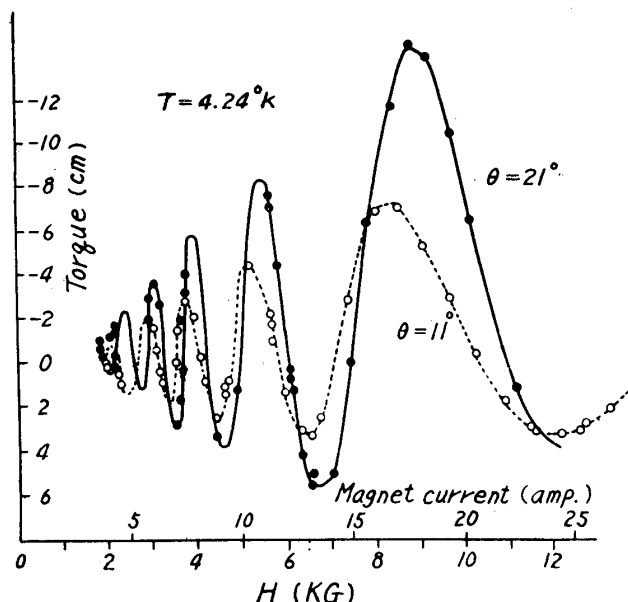


Fig. 7. Long-period effect at 4.24°K; the curves point upwards with increasing field owing to the fact that the torque is proportional to  $H^2$ .

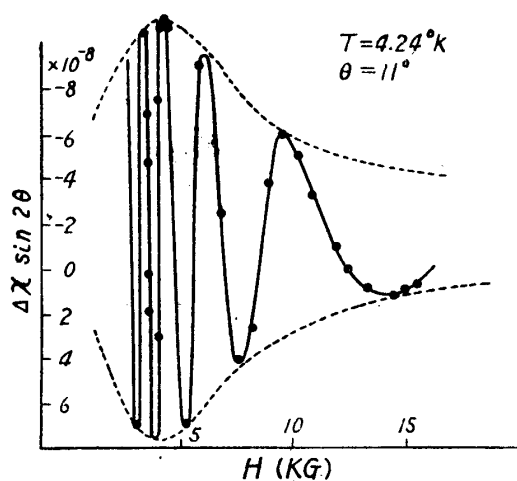


Fig. 8. Long-period effect ( $\Delta\chi \sin 2\theta$  vs.  $H$ ) at 4.24°K and  $\theta = 11^\circ$ .

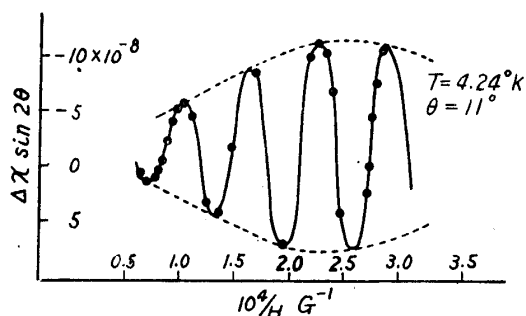


Fig. 9. Long-period effect ( $\Delta\chi \sin 2\theta$  vs.  $1/H$ ) at 4.24°K and  $\theta = 11^\circ$ .

results obtained for  $\theta = 21^\circ$  and  $11^\circ$  are shown in Fig. 7. At this temperature range, the effect becomes well marked and the number of peaks indicating the period increases, so that considerably definite inferences become possible. Fig. 8 shows the curve  $\Delta\chi \sin 2\theta$  vs.  $H$  for  $\theta = 11^\circ$  and Fig. 9 the curve  $\Delta\chi \sin 2\theta$  vs.  $1/H$ . The amplitude increases with the intensity of magnetic field up to the maximum at about 4 kG, but turns to diminish with increasing field beyond that point, becoming markedly small in the range above 16 kG. The period, however, falls off monotonously with the increase of the angle  $\theta$ , in agreement with the result of analysis described below.

3. Fine structure observable in the range of 4.2~1.3°K and above 19 kG (Short-period effect)

Then, the measurements were carried out by varying the angle  $\theta$  between the axis-3 and the field as well as the temperature. The results are shown in Figs. 10 and 11. The values of  $\Delta l/H^2$  ( $\Delta l$ : the shift of the image) are plotted against the magnetic field taking  $\theta$  as a parameter (cf. Equ. (4)). The steady increasing tendency of the undulatory curves with the rise of the magnetic field is due to the superimposition of the short-period effect upon the extension of the long-period effect,

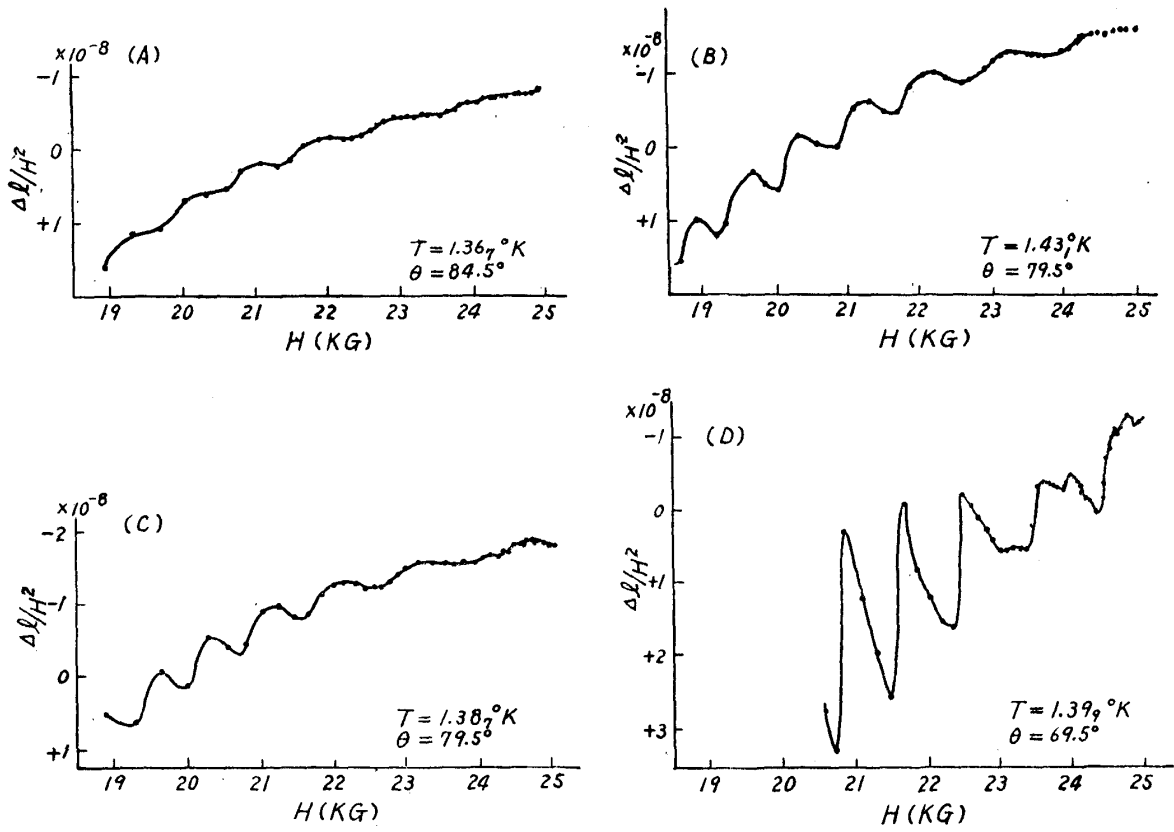


Fig. 10. Short-period effect ( $\Delta l/H^2$  vs.  $H$ ) at about  $1.4^\circ\text{K}$ , when  $\theta$  is varied from  $84.5^\circ$  to  $69.5^\circ$ .

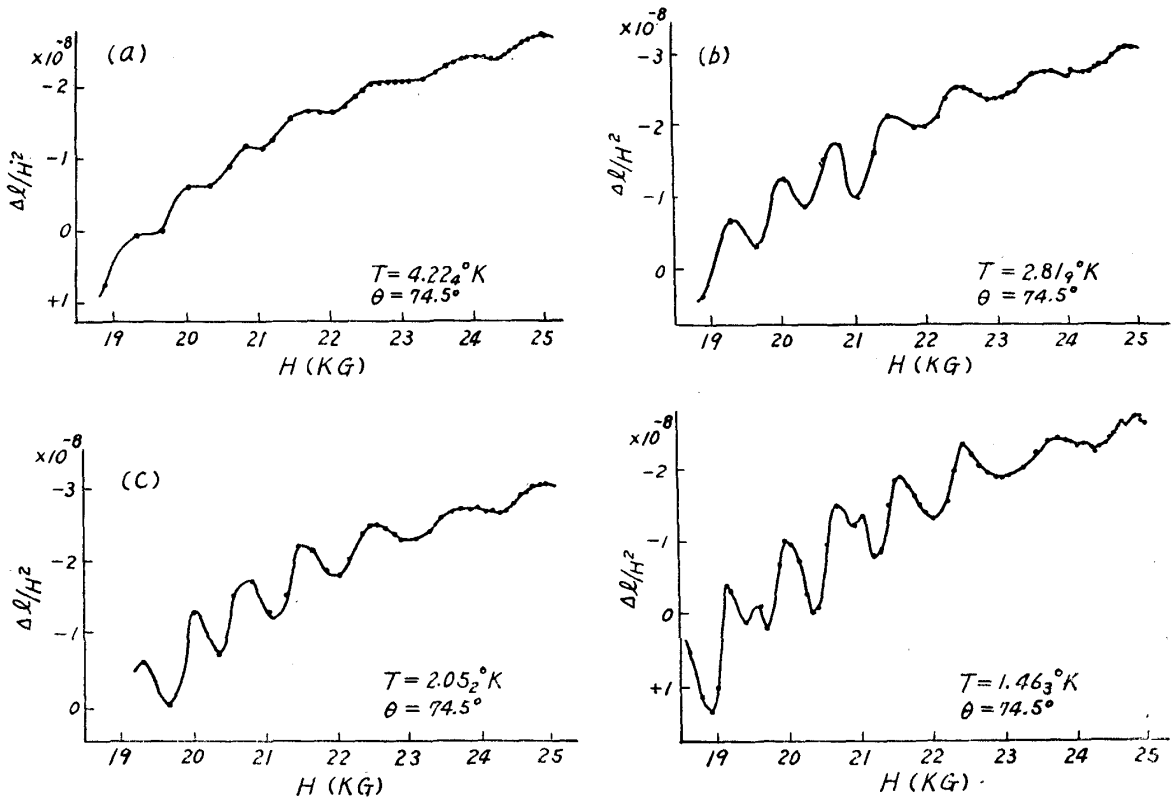


Fig. 11. Short-period effect ( $\Delta l/H^2$  vs.  $H$ ) for  $\theta = 74.5^\circ$ , when temperature is varied from  $4.22^\circ$  to  $1.46^\circ\text{K}$ .

the latter being not so perceptible, though still extant, in this field range. In order to facilitate to envisage the short-period effect alone, the results obtained by replotting these curves against the reciprocal of the field are displayed in Figs. 12, 13 and 14 (full curve), and then by subtracting from them the part ascribable

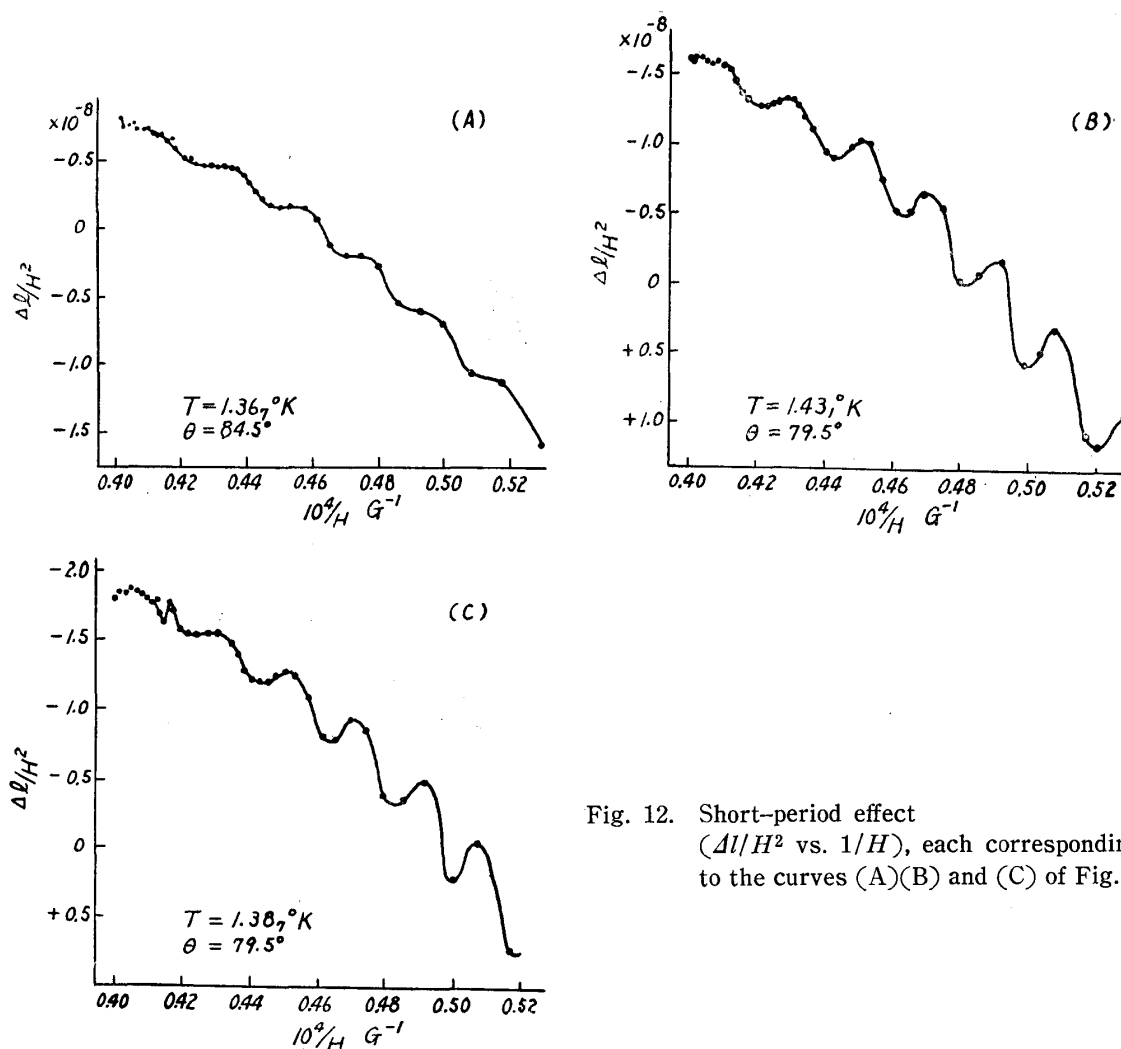


Fig. 12. Short-period effect ( $\Delta l/H^2$  vs.  $1/H$ ), each corresponding to the curves (A)(B) and (C) of Fig. 10.

to the long-period effect are presented in Figs. 14 (broken curve), 15 and 16. In these curves, to some measure, are observed beat-like structures which are highly probable to be resulted from the superposition of two or more oscillations. The beats grow more prominent as the temperature drops and as the angle  $\theta$  is reduced. The augment of the amplitude at lower temperatures may be foreseen from the fact that the lower the temperature the smaller becomes the lattice vibration and consequently the fluctuation of the energy level will be reduced. The relationship between the amplitude and the angle  $\theta$  is opposite to that in the case of the long-period effect, i. e., the amplitude decreases with increasing  $\theta$ . While the period, as described below, increases along with  $\theta$  and in many cases it becomes more or less prolonged towards the high field side. Besides, in certain cases, some anomalies in oscillatory pattern are observed in the vicinity of 22.4 kG ( $1/H = 0.41 \times 10^{-4} \text{ G}^{-1}$ ), the point corresponding to the node of beats. This may

probably be due to the advent of the superfine structures, the period of which is still shorter than the main short-period effect stated above, as they scarcely have become perceptible at this field. But for ascertaining the details on this point, further measurements in stronger fields are not dispensed with.

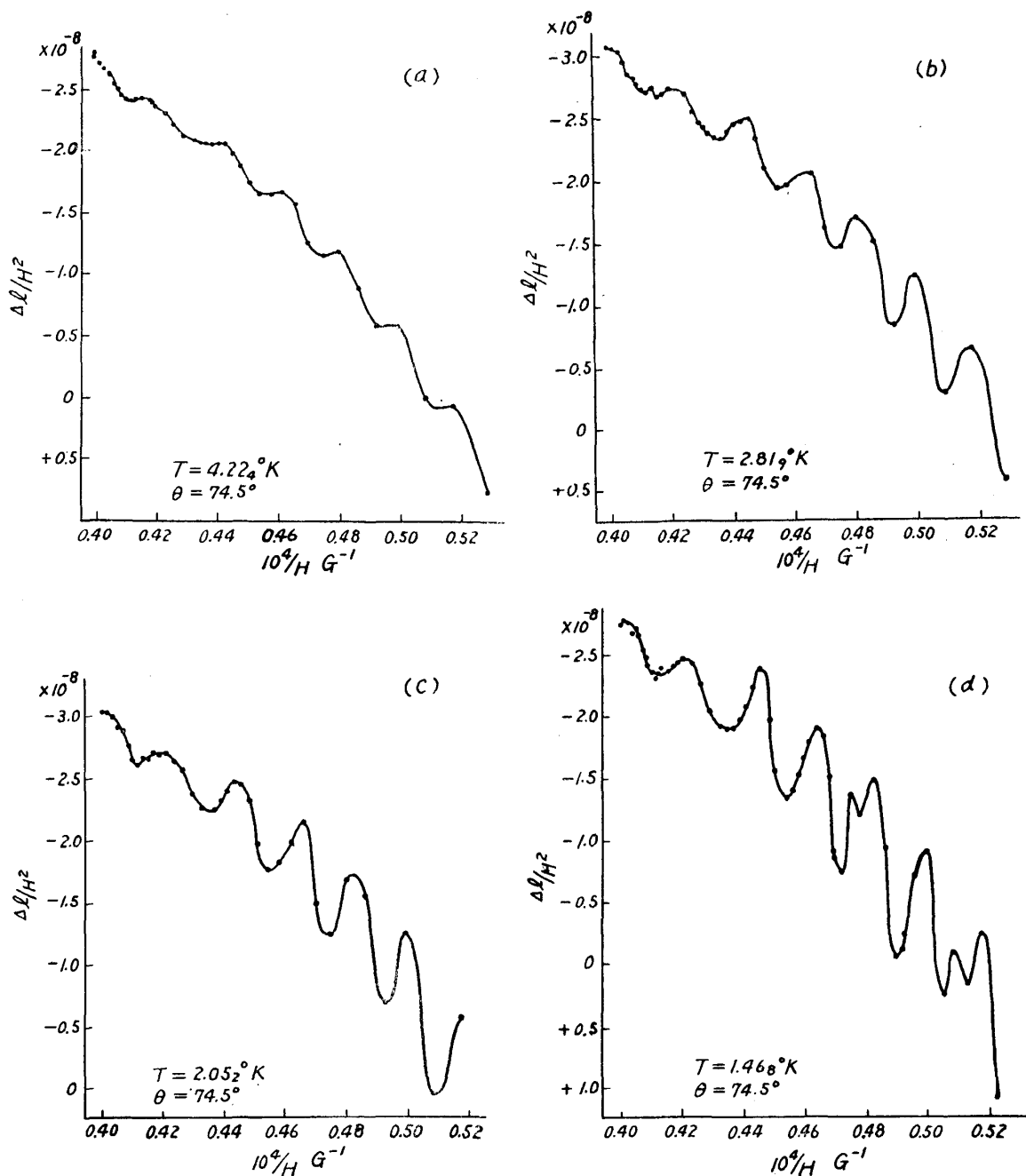


Fig. 13. Short-period effect ( $\Delta l/H^2$  vs.  $1/H$ ) each corresponding to the curves (a), (b), (c) and (d) of Fig. 11.

#### 4. Results of measurements in the vertical position of axis-3 or the anisotropy in the plane of the axes-1 and -2

The results are shown in Fig. 17, but our comments on them will be deferred to the chapter of discussion below.

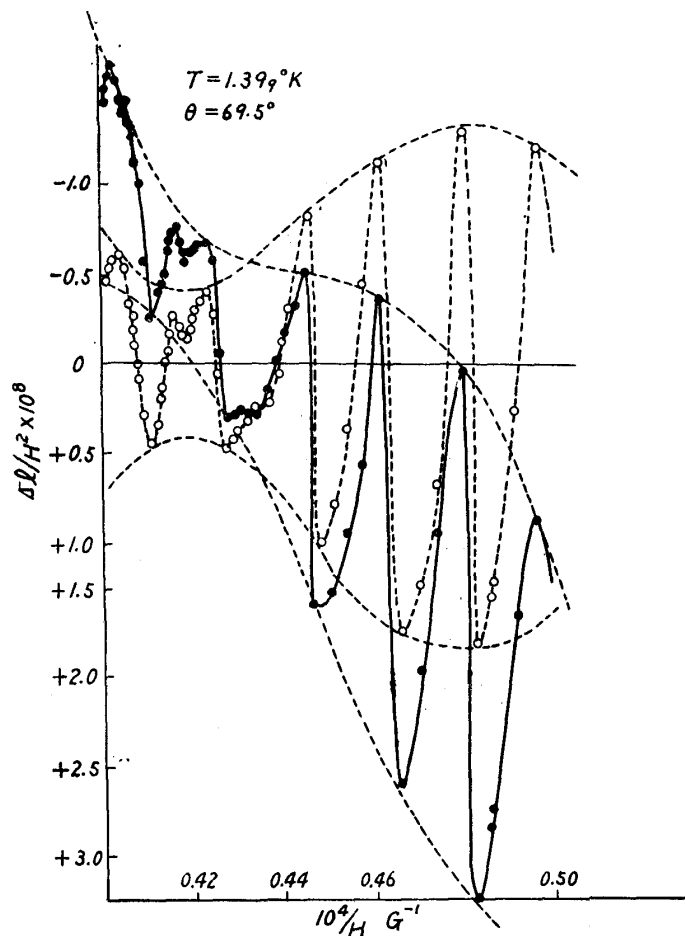


Fig. 14. Short-period effect ( $\Delta l/H^2$  vs.  $1/H$ ), corresponding to the curve (D) of Fig. 10.

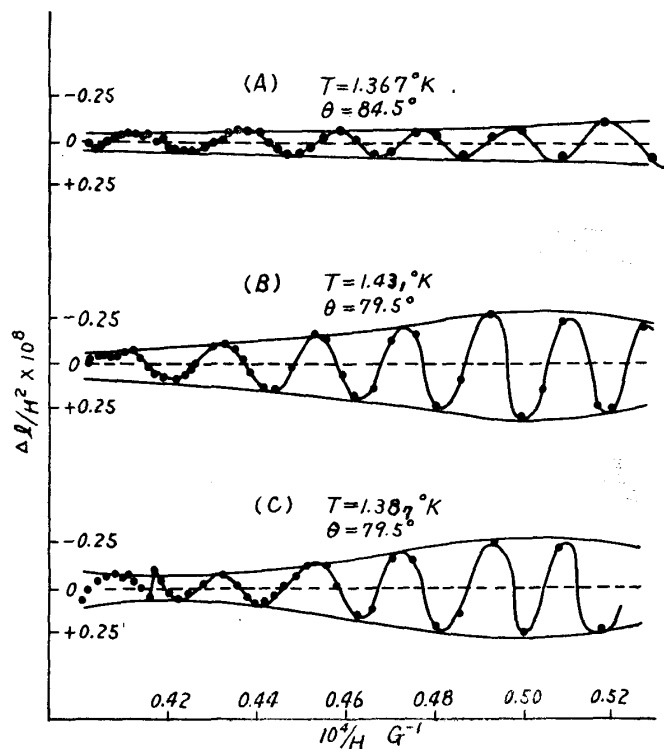


Fig. 15. Short-period effect ( $\Delta l/H^2$  vs.  $1/H$ ) after subtracting the part responsible for, the long-period effect, each corresponding to the curves (A), (B) and (C) of Fig. 12.

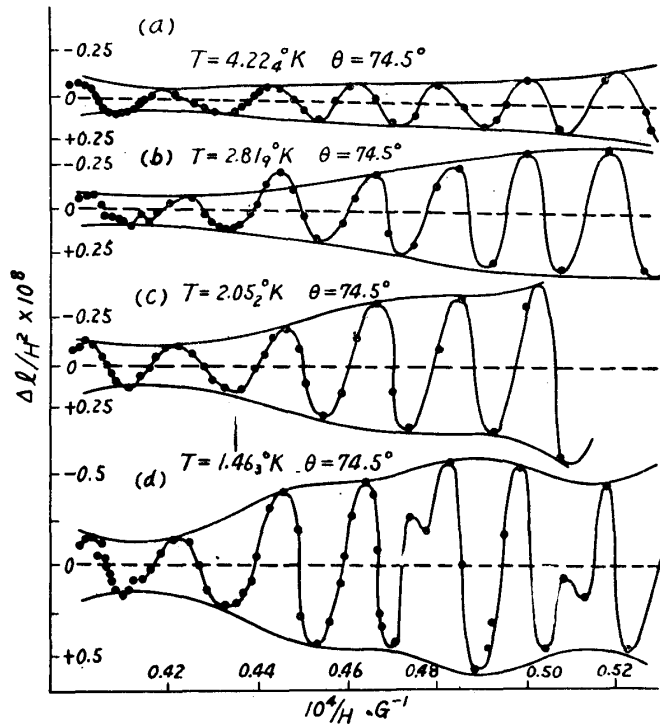


Fig. 16. Short-period effect ( $\Delta l/H^2$  vs.  $1/H$ ) ( $\theta = 74.5^\circ$ ) after subtracting the part responsible for the long-period effect, each corresponding to the curves (a), (b), (c) and (d) of Fig. 13.

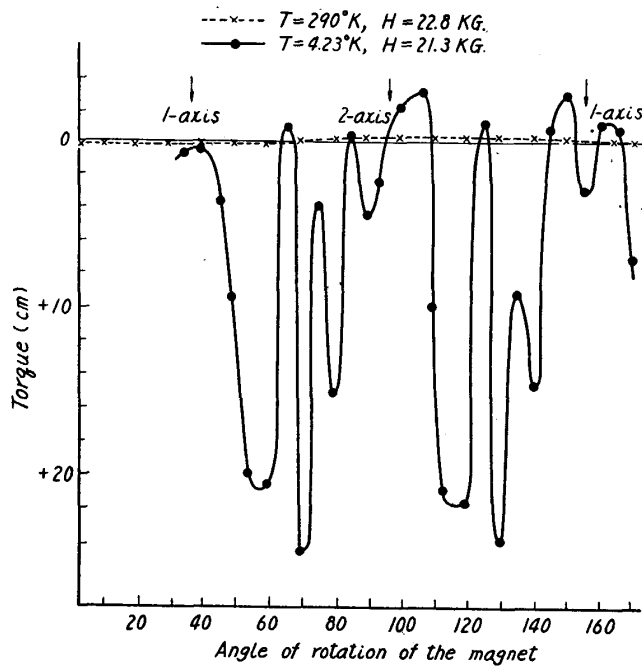


Fig. 17. Torque curves obtained by suspending the sample along axis-3 in the position of Fig. 5 (d), the arrows indicate the direction of axis-1.

#### IV. Discussion of the results

##### 1. Theoretical

It is believed that the dH-vA effect is a universal phenomenon observable in the single crystals of metals. Up to date, however, this oscillatory behaviour has been reported concerning the 14 kinds of metals and graphite, but if the existence of the effect is tested under stronger magnetic fields and at lower temperatures, it is probable that the similar effect would be observed in other metals too. If the theoretical expression cited below is valid, it will be concluded that in case the effective mass and the chemical potential of the charge carriers are smaller for a certain metal, the more easily observable would be the effect. The multi-valent metals, in which the Fermi surface overlaps the Brillouin zone boundary, are generally likely to fulfil these two requirements.

Peierls<sup>(1)</sup>, Blackman<sup>(2)</sup> and Landau<sup>(16)</sup>, starting from a free-electron model, deduced a theoretical formula of the dH-vA effect. In accordance with Landau<sup>(16)</sup>, the expression for the anisotropy  $\Delta\chi$  is given by

$$\Delta\chi = \sum \frac{A\Delta m}{\rho} \left\{ \frac{\pi^2}{6} \left( \frac{k}{E_0} \right)^{1/2} - \frac{1}{T^{1/2}} \left( \frac{2\pi^2 kT}{\beta H} \right)^{3/2} \right. \\ \left. \times \sum_{p=1}^{\infty} \frac{(-1)^{p+1} \sin(2\pi p E_0 / \beta H - \pi/4 \cdot \delta)}{2p^{1/2} \sinh(2\pi^2 kT / \beta H)} \right\}, \quad (5)$$

provided that  $E_0 \gg kT$  and  $E_0 \gg \beta H$ , which is not fulfilled at the highest temperatures or highest fields in the case of long-period effect.  $\rho$  is the density,  $A$  is a constant given by

$$A = e^2 E_0 / \pi^4 c^2 \hbar (2k)^{1/2} m'^{3/2}. \quad (6)$$

$\beta$  is a double effective Bohr magneton given by

$$\beta = e\hbar/m''c, \quad (7)$$

where  $m'$ ,  $m''$  and  $\Delta m$  denote certain functions of the relevant effective masses and  $\theta$ , which values depending on the geometry of the experiment and the shape of the Fermi surface of the metal.  $E_0$  represents the chemical potential measured either from the bottom of the zone which is responsible for the effect in the case of electrons or from the top of the zone in the case of holes.

In many cases, it is possible to represent the Fermi surface of metals by a set of 1, 2 or 3 ellipsoids. The  $\sum$  at the top of the Equ. (5) means the summation with respect to the respective ellipsoids which are characterized by the mutually independent parameters  $m'$ ,  $m''$ . By setting the axes of the specimen in appropriate positions, paying due regards to that remarked above, any one of the ellipsoids can be represented by

$$E_0 = P_1^2/2m_1 + P_2^2/2m_2 + P_3^2/2m_3, \quad (8)$$

(16) L. D. Landau : Appendix of Shoenberg's paper (Proc. Roy. Soc. London, **A170** (1939), 363).

in which  $P$ 's and  $m$ 's designate the momenta and the effective masses in the directions of axes-1, 2 and 3. And if they are equivalent with respect to axes-1 and -2, Equ. (8) becomes

$$E_0 = (P_1^2 + P_2^2)/2m_1 + P_3^2/2m_3. \quad (8')$$

More recently, Onsager<sup>(17)</sup> has pointed out that no essential difference will be occasioned by assuming more general energy surface, for instance, a set of hyperboloid or a cylinder, instead of an ellipsoid. And he deduced the validity of the next relationship

$$\text{Period} = \frac{e}{hcA}, \quad (9)$$

between the period of oscillation and the extreme area,  $A$ , of the cross-section of the Fermi surface cut by the planes normal to the field. Mase<sup>(18)</sup>, taking notice of this proposition, calculated the values with the cases of ellipsoid, hyperboloid and cylindrical energy surfaces and found that everyone of them gives the same period in the first approximation.

## 2. Method of analysis

(i) Dependence of the oscillation period on magnetic field ( $\theta$  and  $T$  being kept constant)

According to the Equ. (5), the undulation reaches the maxima and the minima when the following equation is satisfied:

$$\sin\left(\frac{2\pi E_0}{\beta H} - \frac{\pi}{4} \delta\right) = \pm 1.$$

Therefore, when the peaks of oscillation are numbered  $n$  from high field side and by plotting the corresponding  $1/H$  against  $n$ , we obtain a linear relationship

$$\frac{1}{H} = \left(\frac{\beta}{E_0}\right) \frac{n}{2} + C_1, \quad (10)$$

and hence we can determine the period of oscillation  $\beta/E_0$  as a function of the angle  $\theta$  between the axis-3 and the magnetic field. Moreover, by extrapolating this straight line to the abscissa axis ( $H \rightarrow \infty$ ), we get the value of phase constant  $\frac{\pi}{4} \delta$ . Theoretical point of view expects that  $\frac{\pi}{4} \delta = \frac{\pi}{4}$ , or  $\delta = 1$ , while the experimental results are considerably at variance with this in most cases, the instance of coincidence being rather scarce.

If Equ. (7) is rewritten, by use of Equ. (8'), in the next form as a function of  $m_1$ ,  $m_3$  and  $\theta$ ,

$$\beta = \frac{e\hbar}{cm_1 m_3^{1/2}} (m_1 \sin^2 \theta + m_3 \cos^2 \theta)^{1/2}, \quad (7')$$

and also can be assumed to be  $m_1 \sin^2 \theta \ll m_3 \cos^2 \theta$ , that is to say, the oscillation

(17) L. Onsager, *Phil. Mag.*, **43** (1952), 1006.

(18) S. Mase, *Busseiron Kenkyu* (Japanese) **97** (1956), 1.



period  $(\beta/E_0)$  is obtained by an extrapolation to the case  $\theta \rightarrow 0$ , we get the next relationship

$$E_0 m_1 = 1.689 \times 10^{-47} / (\beta/E_0)_{\theta \rightarrow 0}. \quad (11)$$

(ii) Temperature dependence of amplitude ( $H$  and  $\theta$  being kept constant)

$\beta$  can be deduced from the temperature dependence of the amplitude. By taking logarithm of both sides of Equ. (5) and rearranging, we obtain

$$\log\left(\frac{a}{T}\right) + C_2 = -\gamma\left(\frac{2\pi^2 k}{\beta H}\right) T - \log\left(1 - e^{-\frac{2\pi^2 k T}{\beta H}}\right), \quad (12)$$

where the amplitude  $|a| = \frac{(m_1 - m_3)A}{\rho} \frac{1}{T^{1/2}} \left(\frac{2\pi^2 k T}{\beta H}\right)^{2/3} \exp\left(-\frac{2\pi^2 k T}{\beta H}\right)$  and  $\gamma = \log_{10} e$ .

Thus, by plotting  $\log\left(\frac{a}{T}\right)$  vs.  $T$ , we can compute its gradient  $2\pi^2 k/\beta H$  and hence the value of  $\beta$ . The reason is that in Equ. (12), the second term of right-hand side member  $\log\left(1 - e^{-\frac{2\pi^2 k T}{\beta H}}\right)$  is nearly zero, so far as the condition  $2\pi^2 k T \gg \beta H$  is met, so that this term may be neglected.

(iii) Dependence of amplitude on the magnetic field ( $T$  and  $\theta$  being kept constant)

In a quite similar way,  $\beta$  can be computed from the dependence of the amplitude on the magnetic field. To express the relation between the amplitude  $a$  and the magnetic field  $H$ , we can deduce the following equation akin to Equ. (12) above:

$$\log(aH^{3/2}) - C_3 = -\gamma\left(\frac{2\pi^2 k T}{\beta}\right) \frac{1}{H} - \log\left(1 - e^{-\frac{2\pi^2 k T}{\beta H}}\right), \quad (13)$$

and hence the curve of  $\log(aH^{3/2})$  vs.  $1/H$  gives the value of  $\beta$  in terms of its gradient.

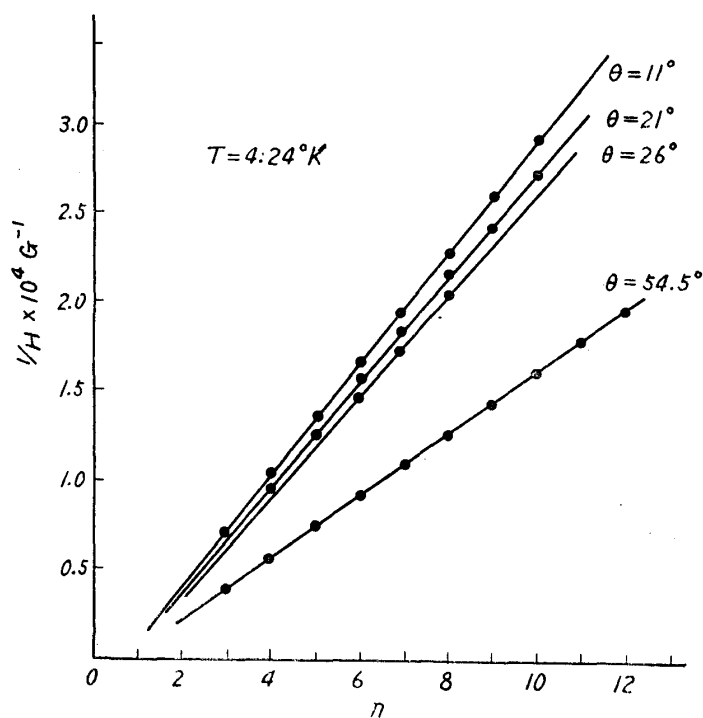


Fig. 18. Long-period effect  $n$  vs.  $1/H$ .

### 3. Results of analysis and discussion

In Fig. 18 are shown the curves  $n$  vs.  $1/H$  for determining the long-period  $(\beta/E_0)_l$  and the results in Table 2 are thus obtained. The short-period  $(\beta/E_0)_s$  in Table 3 are gotten in the same ways. Where the suffixes  $l$  and  $s$  are used to designate the attributes of the long- and the short-period effects respectively.

On plotting the curves  $\left(\frac{\beta}{E_0}\right)_l^2$  vs.  $\cos^2 \theta$  for determining the dependence of the long-period on  $\theta$ , we obtain approxi-

mately a straight line as in Fig. 19, by which is meant that the long-period varies with respect to  $\theta$  according to the relation given by Equ. (7'). By extrapolation of  $\theta \rightarrow 0$  or  $\cos^2\theta \rightarrow 1$ , the maximum value of the long-period,  $0.65 \times 10^{-4} G^{-1}$ , is deduced, a value in good agreement with that reported by Shoenberg<sup>(6)</sup> ( $0.7 \times 10^{-4} G^{-1}$ ) and that by Berlincourt and Steele<sup>(13)</sup> ( $0.64 \times 10^{-4} G^{-1}$ ).

Table 2. Long-period effect

$\theta^\circ$	$(\beta/E_0)_l$
11	$6.19 \times 10^{-5} G^{-1}$
21	5.88 "
26	5.68 "
54.5	3.39 "

Table 3. Short-period effect

$\theta^\circ$	$(\beta/E_0)_s$
69.5	$1.86 \times 10^{-6} G^{-1}$
74.5	1.96 "
79.5	2.02 <sub>3</sub> "
84.5	2.06 ,

Moreover, if the values of  $\log(aH^{3/2})$ , in which  $a$  denotes the amplitude of oscillation, are plotted as functions of  $1/H$  for the cases of  $\theta = 11^\circ$  and  $\theta = 21^\circ$ , the linear relationships as in Fig. 20 were obtained as expected from Equ. (13). From these data the values of  $\beta_{l,\theta=11^\circ} = 4.73 \times 10^{-18}$  and  $\beta_{l,\theta=21^\circ} = 3.26 \times 10^{-18}$  are deduced. The parameters obtained in connection with the long-period effect are summarized as follows:

$$E_{0l} = 5.5 \times 10^{-14} \text{ erg},$$

$$\left(\frac{m_1}{m_0}\right)_l = 5.4 \times 10^{-3},$$

$$\left(\frac{m_3}{m_0}\right)_l = 2.7 \times 10^{-1},$$

$$T_{D,l} = 400^\circ \text{K},$$

$$n_l = 1.2 \times 10^{-6} \text{atom}^{-1}.$$

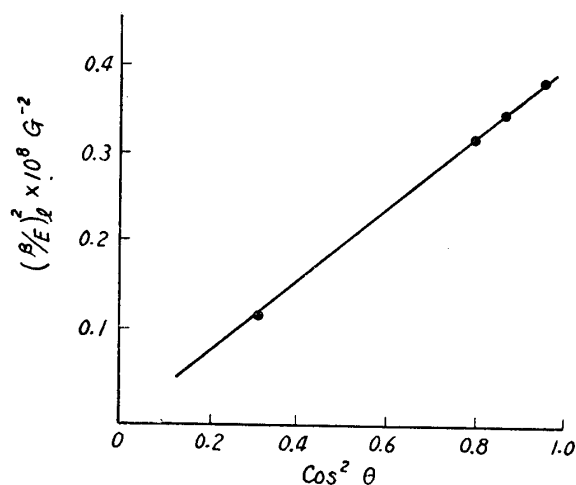


Fig. 19. Long-period effect  $((\beta/E_0)_l)^2$  vs.  $\cos^2\theta$ .

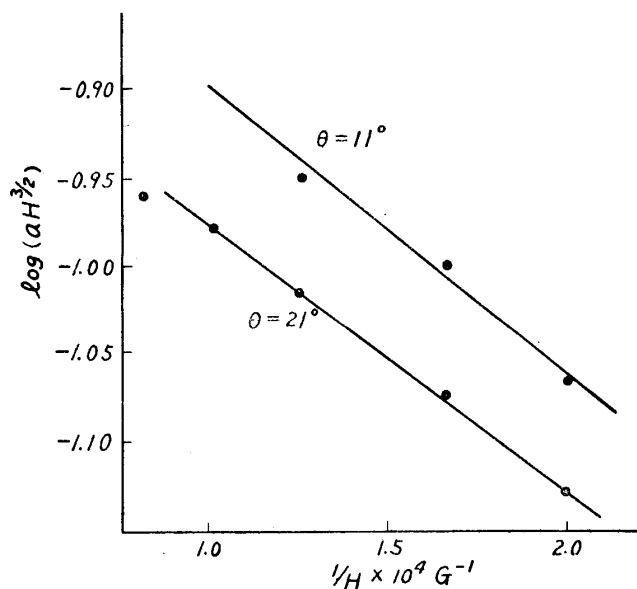


Fig. 20. Long-period effect  $(\log(aH^{3/2}))$  vs.  $1/H$ .

According to the theoretical result deduced from a free-electron model, the amplitude of oscillation versus the magnetic field is expected to decrease exponentially with rise in temperature, so that at high temperatures, as  $T = 63^\circ\text{K}$ , it should be considerably reduced as small as about  $1/16$  of that at  $4.2^\circ\text{K}$ . In our experimental results, however, it has only reduced to about  $1/8$ .

The same applies also to the period. Namely, on comparing the period  $\beta/E_0$  at  $4.2^\circ\text{K}$  and at  $63^\circ\text{K}$ , we found that the latter is about twice the former. The above two observations lead us to infer that the chemical potential  $E_0$  or/and the double effective Bohr magneton would be dependent on temperatures. This inference, however, is applicable only when a free-electron model is adopted. When the electric field and the magnetic field in the crystal are treated as equivalent, it had been also suggested by Harper<sup>(19)</sup> that, in the case of the overlapping bands, a free-electron approximation is not appropriate. But Berlincourt and Steele<sup>(13)</sup> tried to explain this problem qualitatively, with some success, by taking into account the thermal expansion of the crystal lattice.

In the case where the periodicity can be expressed by oscillation terms of one kind alone, the above method for determining  $\beta$  is applicable, but where it consists of composite terms involving several kinds of oscillation terms the situation becomes more complicated. In principle, the component amplitudes and periods of the oscillation terms should be determined by the analysis of modulation, that is, the harmonic analysis of the beat. But as the exponential term begins to affect the results rather heavily, good results can hardly be expected were it not for a sufficient number of beats could be observed. Although it may be feasible to analyse our results into a number of oscillation terms, the number

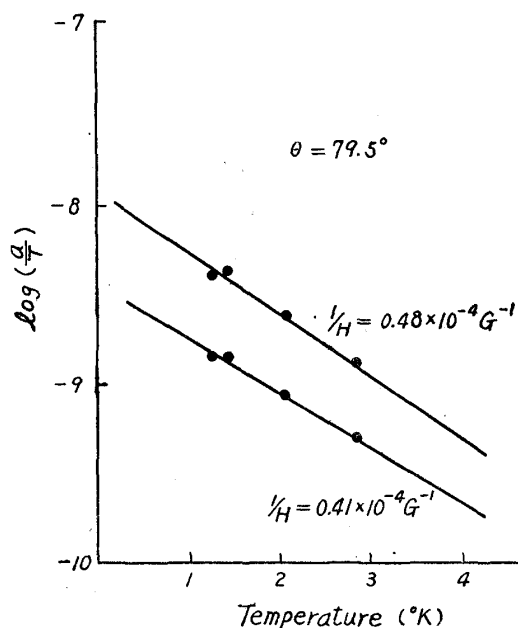
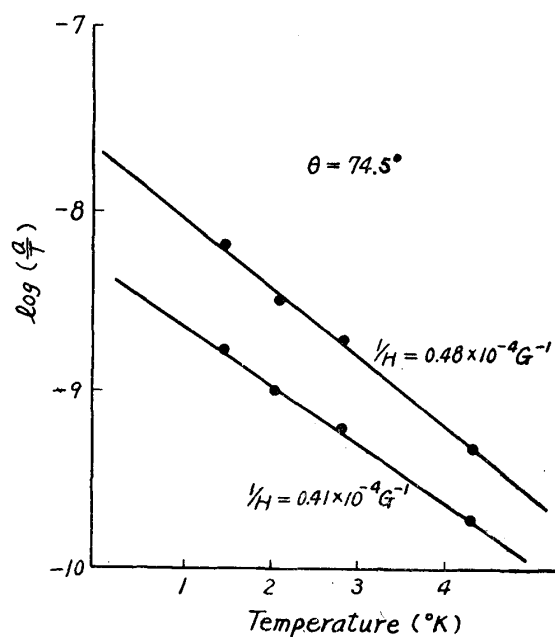


Fig. 21(a). Short-period effect ( $\log a/T$  vs.  $T$ ).

Fig. 21(b). Short-period effect ( $\log aT$  vs.  $T$ ).

(19) P. G. Harper, Proc. Phys. Soc. B68 (1955), 874; 879.

of beats seems to be not sufficient enough to compute the accurate values of the parameters.

But in the case where one of the oscillation terms is presumably predominant over the others, it would cause no perceptible error even if we assume that the amplitude of the composite term is almost determined by that of the dominant term. In compliance with this inference, we determined  $\beta_s$  from the temperature dependence of the amplitude as presented in Fig. 21 (a), (b), postulating that  $\beta_s$  can be deduced from Equ. (12). The parameters for the short-period effect are listed as follows:

$$E_{0,s} = 7.9 \times 10^{-14} \text{ erg},$$

$$\left(\frac{m_1}{m_0}\right)_s = 1.6 \times 10^{-1},$$

$$\left(\frac{m_3}{m_0}\right)_s = 8.3 \times 10^{-2},$$

$$T_{D,s} = 570^\circ \text{K},$$

$$n_s = 3.0 \times 10^{-5} \text{ atom}^{-1}.$$

The torque acting on the crystal positioned as in Fig. 5 (d), i. e. when the axis-3 is set vertical, is expressed by putting  $\theta \rightarrow \theta'$ ,  $\phi \rightarrow 0$  and  $\psi \rightarrow 90^\circ$  in Equ. (1) as below

$$C = \frac{1}{2}(\chi_1 - \chi_2)H^2m \sin 2\theta',$$

where  $\theta'$  stands for the angle between the axis-1 and the magnetic field. Therefore in hexagonal metals, considering the symmetry of the crystal, a 6-cycled torque curve should result during a complete revolution. Provided, however, that the condition  $\chi_1 = \chi_2$  is met, no torque should appear at any value of  $\theta'$ . The actual observations are displayed in Fig. 17, the ordinate indicating the torque measured by the mirror deflection in cm and the abscissa the angle. The arrow marks in the figure indicate the directions of the axis-1. The broken line shows the results measured at room temperatures. The slight fluctuation of  $180^\circ$  period observed in the curve at room temperatures is to be ascribed to the component torque due to the projection of the axis-3 to the horizontal plane, since the axis-3 is not exactly vertical but is inclined by about  $0^\circ 40'$ . Seeing that no 6-cycled torque appears in the result obtained at room temperatures, we can conclude that  $\chi_1 = \chi_2$  at room temperatures. Next, as the results of measurement at liquid helium temperatures, while keeping the crystal at perfectly identical position, four remarkable oscillations are observed for every period of  $60^\circ$  rotation. Hence, it is deduced that a considerable anisotropy exists in the plane of axes-1 and -2 in the range of very low temperatures. The repetition of similar curves at every  $60^\circ$  interval have, of course, been foreseen from the hexagonal symmetry of zinc. With a view to ascertaining the absence of any torque due to the specimen holder and other parts excepting the specimen, blank tests were

performed without suspending the specimen, the results are that the torque amounting no more than  $5 \times 10^{-11}$  dyne cm/gG<sup>2</sup> has subsisted at the most.

Therefore, it may be concluded that the magnetic susceptibility in the plane of axes-1 and -2 is isotropic at room temperatures, but in the very low temperature range a perceptible anisotropy of six-fold symmetry appears. Sydoriak and Robinson<sup>(11)</sup> asserted that there is no anisotropy in the plane of axes-1 and -2. Berlincourt<sup>(20)</sup> reported that in experimenting with cadmium, having the same six-fold symmetry as zinc, the torque remained in the order of less than  $10^{-11}$  dyne cm/gG<sup>2</sup>, so that no anisotropy could be detected. Therefore, a further investigation in this connection is under way in order to reconcile our experimental results with those of the other authors, since the results in Fig. 17 are not entirely convincing owing to the slight departure from vertical direction of the axis-3.

In conclusion, the present writers wish to express their thanks to Mr. J. Watanabe for his assistance in the preparation of crystal and the determination of crystal orientation. A part of the expenses of this study was defrayed from the Scientific Research Fund allocated by the Ministry of Education.

---

(20) T.G. Berlincourt, Phys. Rev., **94** (1954), 1172.